Journal Pre-proof

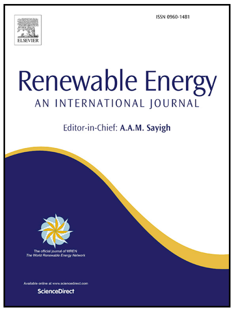

An all-day cooling system that combines solar absorption chiller and radiative cooling

Tianxiang Hu, Trevor Hocksun Kwan, Gang Pei

PII: S0960-1481(22)00068-4

DOI: https://doi.org/10.1016/j.renene.2022.01.058

Reference: RENE 16509

To appear in: *Renewable Energy*

Received Date: 25 August 2021

Revised Date: 26 November 2021

Accepted Date: 15 January 2022

An All-day Cooling System that Combines Solar Absorption Chiller and Radiative Cooling

[1]Tianxiang Hu (htx@mail.ustc.edu.cn), [1]Trevor Hocksun Kwan* (trobby@ustc.edu.cn), [1]Gang Pei* (peigang@ustc.edu.cn)
*Corresponding Authors
[1]Department of Thermal Science and Energy Engineering, University of Science and Technology of China, China

Abstract: Although the solar-powered absorption chiller is recently a trending technology for space cooling of buildings, it requires a bulky thermal storage device and complex installations to achieve all-day cooling. In this paper, a new system that couples the solar-driven absorption chiller and radiative sky cooling is proposed to realize 24-h continuous cooling with less floor space and smaller thermal storage. This system involves a specialized module that utilizes the medium temperature flat panel solar collector on its top layer and a selective radiative cooling absorption layer on the bottom layer; The top layer faces the sky during the daytime to collect solar thermal energy to drive the absorption chiller, and it will be flipped to the bottom layer at nighttime to realize radiative cooling. The proposed system is analyzed by coupling the steady-state models of each subsystem and a cooling load model, which are later applied to evaluate the cooling performance under varying weather conditions within a day. The simulation results show that the system can stably meet the cooling demand of 70 m^2 room while only needing half the floor area and a thermal storage tank that is 4 times smaller than the traditional PT-AC system.

Keywords: Solar Absorption Chiller; Radiative Cooling; All-day Cooling; Selective Absorption Coatings

Nomenclature:

Abbreviations

COP – Coefficient of Performance
PT – Photothermal
RSC – Radiative Sky Cooling
AC – Absorption chiller
ARP – Alternating period of refrigeration
FPSC – Flat plate solar collector

Variables

A –Area (m^2)
Q – Heat (W)

An All-day Cooling System that Combines Solar Absorption Chiller and Radiative Cooling

[1]Tianxiang Hu (htx@mail.ustc.edu.cn), [1]Trevor Hocksun Kwan* (trobby@ustc.edu.cn), [1]Gang Pei* (peigang@ustc.edu.cn)
*Corresponding Authors
[1]Department of Thermal Science and Energy Engineering, University of Science and Technology of China, China

Abstract: Although the solar-powered absorption chiller is recently a trending technology for space cooling of buildings, it requires a bulky thermal storage device and complex installations to achieve all-day cooling. In this paper, a new system that couples the solar-driven absorption chiller and radiative sky cooling is proposed to realize 24-h continuous cooling with less floor space and smaller thermal storage. This system involves a specialized module that utilizes the medium temperature flat panel solar collector on its top layer and a selective radiative cooling absorption layer on the bottom layer; The top layer faces the sky during the daytime to collect solar thermal energy to drive the absorption chiller, and it will be flipped to the bottom layer at nighttime to realize radiative cooling. The proposed system is analyzed by coupling the steady-state models of each subsystem and a cooling load model, which are later applied to evaluate the cooling performance under varying weather conditions within a day. The simulation results show that the system can stably meet the cooling demand of 70 m^2 room while only needing half the floor area and a thermal storage tank that is 4 times smaller than the traditional PT-AC system.

Keywords: Solar Absorption Chiller; Radiative Cooling; All-day Cooling; Selective Absorption Coatings

Nomenclature:

Abbreviations

COP – Coefficient of Performance
PT – Photothermal
RSC – Radiative Sky Cooling
AC – Absorption chiller
ARP – Alternating period of refrigeration
FPSC – Flat plate solar collector

Variables

A –Area (m^2)
Q – Heat (W)

U – Heat loss coefficient (W/(m2·K))
F' – Collector's efficiency factor
F_R – Collector's heat removal factor
I – Solar radiation (W/(m2))
V – Velocity (m/s)
h – Heat transfer coefficient (W/(m^2·K))
T – Temperature (K)
k – Thermal conductivity of air (W/(m • K))

Greek symbols

η – Efficiency
ε – Radiative emissivity
λ – Wavelength (nm)
τ – Transmittance
α – Absorptivity

Subscripts

amb – Ambient
bot – Bottom
sky – Sky
ave – Average
f – Fluid
i – Inlet
o – Outlet
s – Solar energy
m – Mean
top – Top
$side$ – Side
L – Loss
$Load$ – Load
E – Evaporator
G – Generator
b – Black body

Constants:

$\sigma = 5.67 \times 10^{-8}$ $\mathrm{W/(m^2K)}$ – Stefan Boltzman constant

1. INTRODUCTION

The demand for energy by humanity has increased dramatically with population growth and the development of science and technology. However, this has worsened environmental problems such as the intensifying greenhouse effect due to increased fossil fuel consumption. In particular, building cooling (including services and households) occupies a very significant part of the total energy demand [1], which may be up to 40% globally or 37% in China [2]. Therefore, the use of renewable energy, such as solar energy [3, 4], for building cooling and temperature regulation has become an increasingly important practice, so governments of various countries are currently promoting research on solar energy utilization [5, 6].

Currently, the heat pump is the most widely used method of refrigeration, but they do have various disadvantages. For example, despite being very widely used in air conditioners, the vapor compression cycle (VCC) involves refrigerants that can significantly damage the natural environment when leaked into it. The thermoelectric cooler (TEC) has a simpler structure and does not require moving mechanical parts, but its cooling performance is insufficient for buildings [7]. Hence, the absorption chiller (AC) is another emerging cooling technology. Despite having a relatively low cooling performance over the VCC, the AC can utilize lower grade heat to produce cooling energy, so it can be easily coupled to a solar collector or a certain facility that produces significant heat [8]. Meanwhile, passive cooling methods such as radiative sky cooling (RSC) have also been favored by many researchers because they do not require any energy consumption [9-11], but their specific cooling capacities are too low for economical use. Overall, optimizing the AC and RSC in terms of their designs and method of operation is an essential step for drawing these technologies closer to widespread commercial use.

One important aspect of solar-driven absorption chillers is the appropriate working solution within the thermodynamic system. A comparative study of different possible solutions was conducted by Kim et al. [12], who found that the total cost of a single-effect LiBr-H_2O absorption system was the lowest. This finding is consistent with that by Ahmed et al. [13] who evaluated the performance of an integrated cooling plant having both a free cooling system and solar-powered single-effect LiBr-H_2O based AC. Alternatively, other researchers also considered trying to apply a higher temperature solar heat collector as the heat source, which would generally require the use of multi-effect ACs. Specifically, Xu et al. [14] compared different Compound Parabolic Concentrator based solar absorption cooling systems with single, double, and multiple effect absorption chillers. Although this study proved that the double effect AC can allow a higher input temperature and hence yield higher COPs, the system complexity significantly increases, and the increased temperature difference relative to the ambient may cause slower dynamic responses. Actually, the single effect AC is proven to still be an acceptable choice by Azhar et al. [15] even under the harsh hot and humid climatic conditions of New Delhi. Hence, this paper will maintain the use of single effect ACs.

Besides solar energy, another cooling energy source in the sky is using the deep outer space as a heat sink, which is achieved by radiative sky cooling (RSC) [10, 11, 16]. Notably, RSC is a critical heat flow component in the Earth's heat budget system as a means to remove the incoming solar irradiation energy and balance the earth's surface temperature to habitable levels [10]. In regards, a specific RSC module aims to adopt a material with minimized solar irradiation absorption and maximized emissivity in the infrared band so that an environment with a temperature lower than ambient can be generated. To realize the above aims, the appropriate selective absorption coatings choice is critical. As Figure 1 shows, the selective absorbing coatings have high emissivity in the "atmospheric window" band (8 μm to 13 μm) so that infrared energy can radiate into the outer space efficiently. In a recent study of the RSC, an example material is an integrated photonic solar reflector and thermal emitter as introduced by Raman et al. [17], which could reflect 97 percent of incident sunlight while emitting strongly and selectively in the 8 μm to 13 μm window. As a result, the cooler managed to create a 4.9□ below ambient temperature difference even when more than 850 W/m^2 of solar irradiation was incident. Zhao et al. [18] used a low-cost radiative cooling metamaterial to cool water to 10.6□ below ambient temperature. Nevertheless, despite these significant breakthroughs, the RSC has a low cooling capacity so it requires large amounts of material to realize building cooling. This issue is especially detrimental for daytime radiative sky cooling because their required materials are very specialized and expensive to manufacture [1, 19]. As a result, RSC is commonly regarded as an uneconomical option for the building cooling application.

Recently, achieving the RSC and solar thermal functions adaptively with a single panel (PT-RSC) is another recently emerging technology that aims to maximize the usage of the panel throughout the day; During the daytime, the panel converts solar energy into heat, and during the nighttime, the same panel is used to achieve RSC. To achieve this, Hu et al. [19] proposed a hypothetical solar heating and radiative cooling (SH-RC) surface and compared it with traditional solar selective absorbing coating surface (SH surface), spectrally selective radiative cooling surface (RC surface), and spectrally nonselective black surface (SH-RC$_{black}$ surface). Hu et al. [20] later proposed a dual-function collector with heating during the day and cooling at night, and made a photothermal radiation cooling model, and carried out experimental research under heating and cooling modes. Results showed that the collector can get a good daily heat of 8.64 MJ during a consecutive 8 h and a good nightly cooling energy of 0.99 MJ in a consecutive 11.5 h. However, the PT-RSC has a major temporal mismatch issue; The produced daytime heat and nighttime cooling energy are completely opposite to the typical cooling demand profile of the day, so large and costly thermal storage devices are generally needed to realize the PT-RSC system's practical potential.

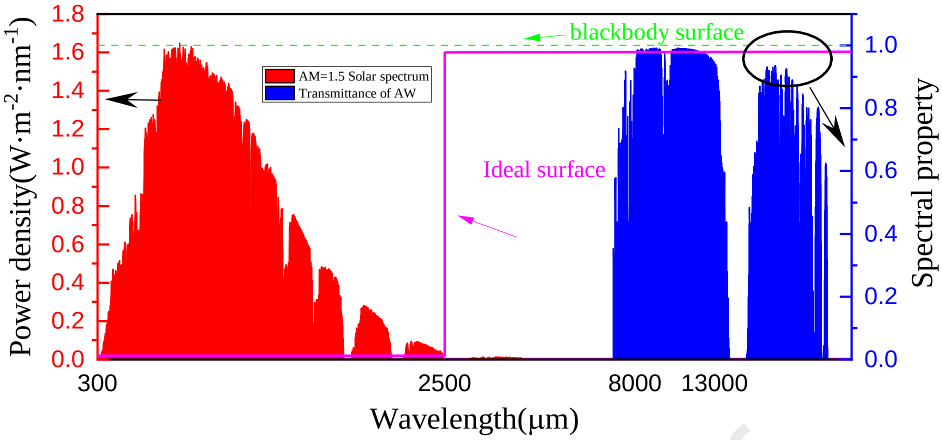

Figure 1: Ideal emissivity of selectivity coatings

Although solar absorption chiller (AC) and radiative sky cooling (RSC) have developed maturely, especially AC has been used widely in people's daily life and industry production [21, 22], they still have their shortcomings. In the solar-driven absorption chiller, large energy storage devices are generally required to support nighttime operation and realize 24-h continuous cooling [23, 24]. Otherwise, due to the volatility of solar energy, especially the lack of energy sources at night, other high-grade heat sources may be needed to avoid the situation that the PT-AC system cannot provide nighttime cold energy. In this regard, because the RSC's operation is optimal during the nighttime and does not require additional input energy, its integration into the solar-driven absorption chiller is expected to greatly alleviate the aforementioned drawback. Thus, this paper proposes to combine the RSC with solar-driven AC functions to achieve all-day cooling while reducing the need for thermal storage. During the daytime, PT-AC works to convert solar energy into heat via a heat transfer fluid (HTF), which is later transferred to the AC to produce cooling energy. Then, during the nighttime, the PT panels will be reversed to radiate infrared energy through the bottom layer that is coated with a selective absorbent coating. Compared with the traditional PT-AC and PT-RSC systems that require a thermal storage tank to realize the all-day cooling, the PT-AC-RSC system can reduce the floor space and the initial system equipment investment. In this way, RSC and PT-AC are integrated to avoid preparing separate sites for these two devices, which greatly reduces the demand for land. In addition, the added RSC enabled the new system to better withstand the drastic changes in solar energy and thermal load, thus showing better stability. The proposed system has been studied by analyzing its ability to meet a continuous cooling demand of a typical home in summer conditions. Several system working parameters have been parametrically studied to assess the factors that can enable the highest system performance.

2.SYSTEM MODELING

Figure 2 shows the overall structure of the PT-AC-RSC system, which works differently between the daytime and nighttime periods. During the daytime, the PT-RSC converts the solar energy into the heat that drives the AC and ultimately produces cooling energy.

When the solar radiation is lower than the driving solar radiation (I_d) of AC, the AC stops functioning and the RSC takes place to produce cooling energy via infrared radiation into the sky. To realize this, the bottom plate is coated with an absorber selective material, and the PT panel should be physically rotated 180 degrees because this coating causes large heat losses during daytime operation of absorbing solar energy. The working process of each model was simulated by MATLAB.

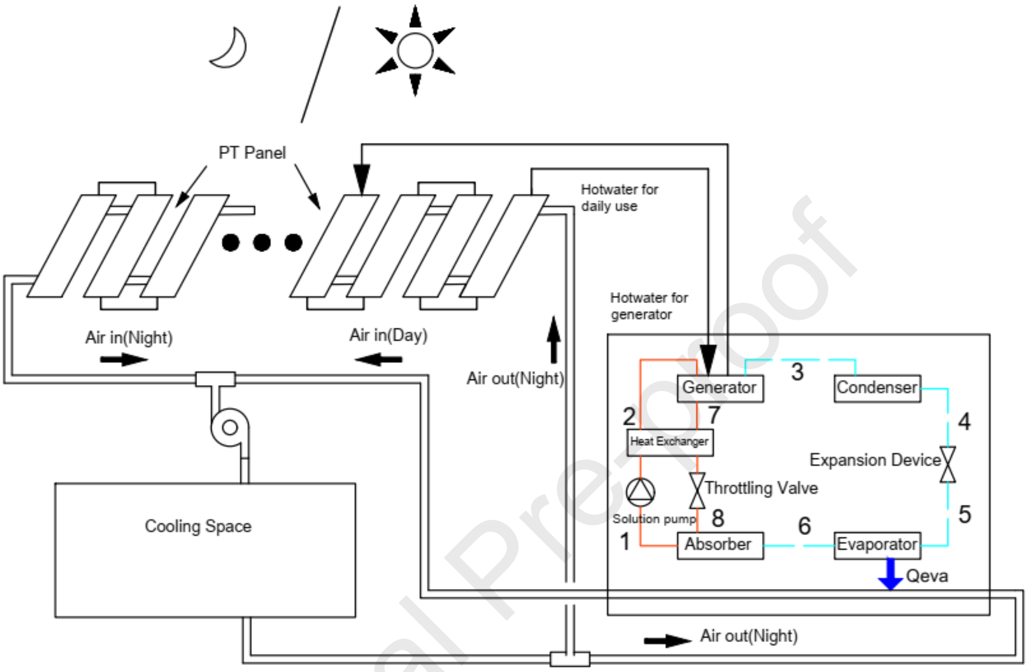

Figure 2: Schematic of the PT-AC-RSC system

The analyzes are conducted with respect to the time of day and the timestep is set to 1 hour. To simplify the analysis, it is assumed that the solar irradiation, cooling demand/supply, and other working parameters are constant during each hour. In this manner, the constant working conditions are inputted to the developed steady-state models to calculate the working status and heat flows of the PT-AC-RSC system at each time step. These steady-state models are described in detail in the following subsections.

2.1 Photothermal and radiative sky cooling model

Figure 3 shows the structure of the flat plate solar collectors (FPSC) of the PT-RC model. From top to bottom, the structure consists of the glass cover, absorber plate, fluid pipe, and bottom plate. As the RSC causes problems to the FPSC's solar thermal performance, the following measures are imposed on the FPSC.

1. The coating on the absorber plate has a high absorptivity in the solar band and very low emissivity in the other wavelength bands.
2. The coating on the bottom plate has a very high emissivity in the infrared band, especially in the "atmospheric window". When the solar irradiance magnitude is no longer sufficient to maintain the AC's operation, the FPSC is flipped 180 degrees to make this coating face the sky and initiate the RSC operation.
3. A vacuum environment is imposed between the glass cover and absorber plate as

well as between the absorber plate and insulator to reduce heat loss. An air gap also exists between the insulator and the bottom plate, which allows the cooling energy from the RSC to be carried into the room by flowing air.

4. It is assumed that the insulator temperature equals the absorber temperature.

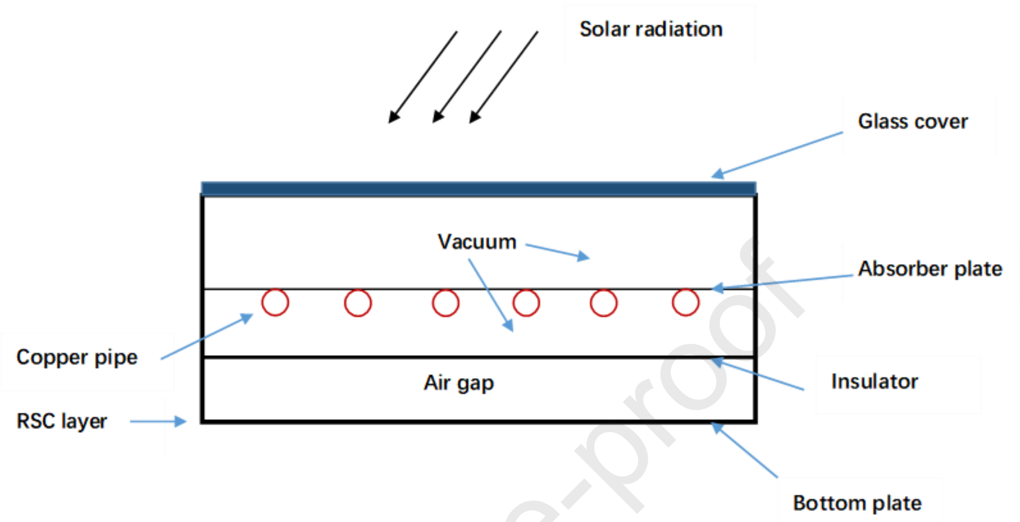

Figure 3: Schematic of the EFPC

2.1.1 Mathematical model of the photothermal

According to the law of energy conservation, the energy used for water heating (Q_h) is equal to the amount of solar energy (Q_s) absorbed minus the heat loss (Q_L) of the collector to the ambient environment:

$$Q_h = Q_s - Q_L \tag{1.}$$

where Q_L includes the heat loss at the top (Q_{top}), the heat loss at the side (Q_{side}) and the heat loss at the bottom Q_b.Therefore, Q_L can be expressed as:

$$Q_L = Q_{top} + Q_{side} + Q_b = A_{top}U_{top}(T_{abs} - T_{amb}) + A_{side}U_{side}(T_{abs} - T_{amb}) + A_{bot}U_b(T_{abs} - T_{amb}) \tag{2.}$$

Because the average temperature of the absorber plate T_{abs} is hard to measure, the general practice is to introduce the collector efficiency factor F', and rewrite the above equation into the following form[11]:

$$Q_h = A_{abs}F_R[I\tau\alpha - U_L(T_{f,i} - T_{amb})] \tag{3.}$$

where:

$$F_R = \frac{Mc_p}{A_{abs}U_L}[1 - \exp(-F'A_{abs}U_L/mc_p)] \tag{4.}$$

$$F' = \frac{1}{W[\frac{1}{D_0+(W-D_0)F} + \frac{U_L}{C_b} + \frac{U_L}{\pi D_i h_{f,i}}]} \tag{5.}$$

$$F = \frac{\tanh[\sqrt{\frac{U_L}{\lambda_p \delta_p}}(W-D_0)/2]}{\sqrt{\frac{U_L}{\lambda_p \delta_p}}(W-D_0)/2} \tag{6.}$$

Here, C_b is the thermal conductivity at the joint of the tube and plate, which can be calculated by the following formula:

$$C_b = \frac{k_b b}{\gamma} \quad (7.)$$

where b and γ are the average width and thickness of the welding material respectively; $h_{f,i}$ is the average convective heat transfer coefficient in the tube and can be calculated by:

$$h_{f,i} = (1430 + 23.3(T_{f,m} - 273.15) - 0.048(T_{f,m} - 273.15)^2)V_f^{0.8}D_i^{-0.2} \quad (8.)$$

V_f is the flow velocity in the tube. The average temperature of the heat transfer fluid can be obtained by integrating the temperature along the entire length of the pipe and taking its average. The specific process can be found in [25], and the obtained expression is:

$$T_{f,m} = T_{f,i} + \frac{Q_h/A_{abs}}{F_R U_L}(1 - F_R/F') \quad (9.)$$

Therefore, the outlet water temperature of the PT model can be expressed as:

$$T_{f,o} = 2T_{f,m} - T_{f,i} = T_{f,i} + 2\frac{Q_h/A_{abs}}{F_R U_L}(1 - F_R/F') \quad (10.)$$

In the above equations, U is the heat loss coefficient and U_L means the total heat loss coefficient. These can be obtained by modeling the system in a thermal resistance network, which is shown in Figure 4.

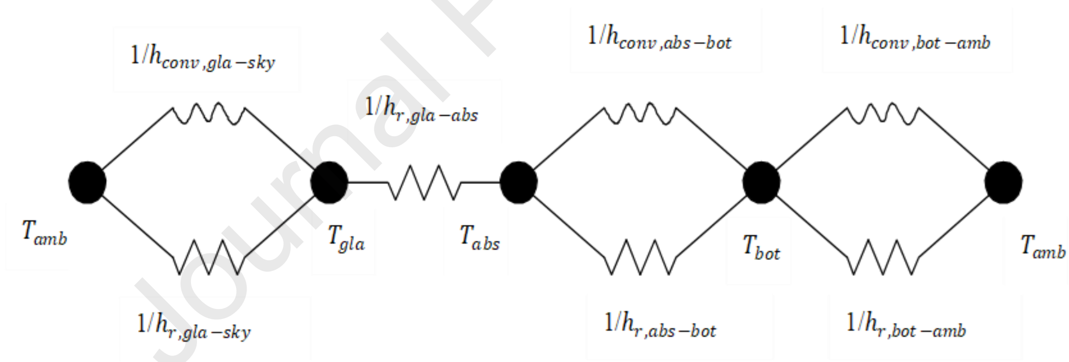

Figure 4: The thermal resistance network diagram

The performance of the PT model can be expressed by the thermal efficiency η_{PT} and its expression is:

$$\eta_{PT} = \frac{Q_h}{A_{abs} I} = F_R \tau\alpha - F_R U_L \frac{(T_{f,i} - T_{amb})}{I} \quad (11.)$$

The above equations can all be solved after setting the relevant physical parameters of the FPSC. Doing so yields the outlet water temperature as needed to evaluate the COP of the AC and the thermal efficiency of the PT model.

2.1.2 Mathematical model of the radiative sky cooling

The PT-RSC model reverses at night so that the bottom faces up for radiative cooling, and the thermal balance of night radiative sky cooling is shown in Figure 5. The net radiative sky cooling power $Q_{net,rad}$ can be calculated as follows (taken from [10, 26]):

$$Q_{net,rad} = Q_{rad} - Q_{r,atm} - Q_{c,atm} - Q_s \quad (12.)$$

where Q_{rad} is the thermal radiation energy; $Q_{r(atm)}$ is the returned radiation energy from the atmosphere; They can be respectively expressed as:

$$Q_{rad} = \int cos\theta d\Omega \int I_{bb}(\lambda, T_s)\varepsilon_s(\Omega, \lambda)d\lambda \quad (13.)$$

and:

$$Q_{r,atm} = \int cos\theta d\Omega \int I_{bb}(\lambda, T_{amb})\varepsilon_s(\Omega, \lambda)\varepsilon_{atm}(\Omega, \lambda)d\lambda \quad (14.)$$

$Q_{c,rad}$ is convective heat transfer with the ambient air, and Q_s is the absorbed solar irradiation power on the surface. Therefore, $Q_{net,rad}$ can be further expressed as:

$$Q_{net,rad} = A_{bot}[\varepsilon\sigma(T_b^4 - T_{sky}^4) + h(T_b - T_{amb}) - \alpha_s I] \quad (15.)$$

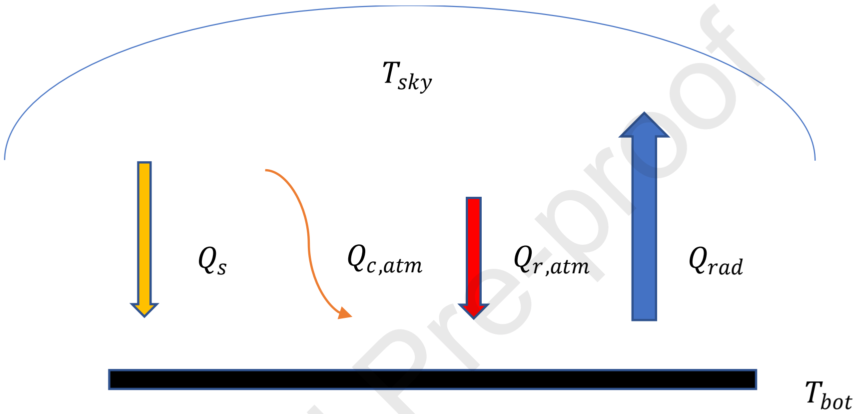

Figure 5: The thermal balance of night radiative sky cooling

where T_{sky} is the effective sky temperature. The researchers have developed some models for calculating the effective sky cooling under clear sky[27, 28]. In this paper, $T_{sky} = 255K$ is imposed, which is consistent with that used in Bergman's work[26]. I is the solar radiation intensity. In the simulation of this paper, the value of I is the solar radiation intensity of Hefei in the first week of August obtained from EnergyPlus[29].

The convection heat transfer coefficient between the bottom and the ambient is often calculated by the following formula [11]:

$$h = 5.8 + 3.8V_{wind} \quad (16.)$$

Notably, one may choose to install a convection shield over the radiative cooling surface to minimize the side effect of convective heat transfer. For example, the RSC module was covered with polyethylene film, a concept proposed by Zhao et al. [30] that changed the heat transfer coefficient to become:

$$h = 2.5 + 2.0V_{wind} \quad (17.)$$

Meanwhile, because the coating of the PT's bottom layer has a high emissivity on the infrared band, the heat loss between the ambient and bottom plate will be higher under the same temperature difference compared with the traditional PT panel. Hence, it is required that the thermal resistance between absorber and bottom plate be maximized, which is dependent on the heat transfer coefficient h_{bi} between the bottom and insulative layers. This parameter is mainly determined based on the thickness of the air gap:

$$h_{bi} = \frac{k}{d_{air}} \tag{18.}$$

where k is the thermal conductivity of air and d_{air} is the thickness of the air gap. For convenience, an idealized spectrally selective surface shown in Figure 1 is assumed for the bottom layer [31]. Specifically, the surface has a high emissivity $\varepsilon_s = 0.95$ only at long wavelengths ($\lambda > 2.5\mu m$, which includes the atmospheric window, $8\ \mu m < \lambda < 13\mu m$) while $\varepsilon_s = 0$ at short wavelengths ($\lambda < 2.5\mu m$). Therefore, the total emissivity ε of the bottom surface, at the temperature T_b is [32]:

$$\varepsilon_{T_b} = \frac{\int_0^{\infty} \varepsilon_\lambda(\lambda.T_b) E_{\lambda,b}(\lambda,T_b) d\lambda}{E_b(T_b)} = \frac{\int_0^{2.5\mu m} \varepsilon_s E_{\lambda,b}(\lambda,T_b) d\lambda}{E_b(T_b)}$$

$$+ \frac{\int_{2.5\mu m}^{\infty} \varepsilon_s E_{\lambda,b}(\lambda,T_b) d\lambda}{E_b(T_b)} \tag{19.}$$

2.2 Mathematical model of absorption chiller

Figure 2 additionally shows the structure of the single effect lithium-bromide absorption chiller (AC) whose operating principle is summarized as follows:

(1) The concentrated solution in the generator will be heated by hot water from the solar collectors. The obtained refrigerant with high temperature and high pressure becomes liquid after passing through the condenser.

(2) After the refrigerant passes through the expansion device and becomes liquid at low temperature and low pressure, it provides cooling energy to the flowing cold air.

(3) Finally, the refrigerant returns to the absorber to be recombined with the solution, which is then pumped to the generator.

(4) There is a heat exchanger between the generator and the absorber. The heat exchange between the concentrated solution and the dilute solution improves the efficiency of energy utilization.

According to the first law of thermodynamics:

$$Q_{eva} + Q_{gen} = Q_{con} + Q_{abs} \tag{20.}$$

The energy balance at the generator yields the following equation:

$$Q_{gen} = \dot{m}_3 h_3 + \dot{m}_7 h_7 - \dot{m}_2 h_2 \tag{21.}$$

The COP of the solar absorption chiller can be calculated as:

$$COP = \frac{Q_{eva}}{Q_{gen}} \tag{22.}$$

where Q_{gen} is the input heat into the AC; $\dot{m}$ is the mass flow rate (kg/s) of the solution or the water, h is the specific enthalpy of the working medium. For the salt solution, h can be calculated according to the reference [26]:

$$h_i = \left(0.0976X_j^2 - 37.512X_j + 3825.4\right)T_i \tag{23.}$$

where X and T are the mass fraction and temperature of the solution, respectively.

According to the ASHRAE Handbook 2013 [33], the evaporation temperature can be obtained in terms of different mass concentrations and pressures of lithium bromide aqueous solutions:

$$T = A_0 + A_1 lnP + A_2(lnP)^2 + A_3(lnP)^3 \tag{24.}$$

In the formula, P is the saturated vapor pressure of LiBr-H_2O and the coefficients A_0,

A_1, A_2, A_4 are:

$$A_0 = a_0 + a_2X + a_4X^2 + a_7X^3$$
$$A_1 = a_1 + a_5X + a_9X^2$$
$$A_2 = a_3 + a_8X$$
$$A_3 = a_6 \tag{25.}$$

Coefficients a_0, a_0… a_9 are regression coefficients obtained by the least-squares regression method respectively, and their values are shown in Table 1.

Table 1: The coefficient values of Equation (22)

n	a_n	n	a_n
0	34.33	5	-16.42
1	18.27	6	0.1108
2	-180.0	7	42.52
3	0.4172	8	0.9320
4	360.1	9	23.10

As for water, the specific enthalpy can be calculated by using a thermophysical properties calculation package such as CoolProp [25]. Thus, the cooling energy produced by AC can be expressed as:

$$Q_{eva} = \dot{m}_6(h_6 - h_5) \tag{26.}$$

In this paper, we first designed an AC model with a rated power of 14 kW. The relevant design parameters are shown in Table 2.

Table 2: Design parameters of AC

Parameters	Value
Rated power	14kW
The inlet temperature of the heat source water	100℃
The inlet temperature of cooling water	31℃
Chilled water inlet and outlet temperature	12℃, 7℃

2.3 Solving the system model

For daytime cooling, when the basic physical parameters such as local total solar radiation I, the inlet water temperature of PT model $T_{PT,in}$, wind speed V_{wind}, ambient temperature T_{amb} are known, the outlet temperature and the cooling energy of the AC can be calculated. This is achieved by the following procedure:

1. Input the known parameters, including $T_{PT,in}$, I, V_{wind} et al into the PT model to

obtain PT outlet water temperature $T_{PT,out}$.

2. Determine whether $T_{PT,out}$ reaches the AC driving temperature T_{drive}. If so, go to step 3, otherwise, return to step 1.
3. Run AC model to obtain the AC outlet water temperature $T_{AC,out}$.
4. Take $T_{AC,out}$ as the new PT inlet water temperature $T_{PT,in,new}$, and run the PT model to obtain the new PT outlet water temperature $T_{PT,out,new}$.
5. Compare $T_{PT,out,new}$ with $T_{PT,out}$, if $T_{PT,out}$ converges, the program terminates, otherwise, go back to step 3.

A numerical simulation program of the model is developed on MATLAB, and the calculation process is summarized in Figure 6. The efficiency of the PT-AC system can be summarized as:

$$\eta_{total} = \frac{Q_E}{A_{abs}I} = \frac{Q_h}{A_{abs}I}\frac{Q_E}{Q_G} = \eta_{PT}COP \quad (27.)$$

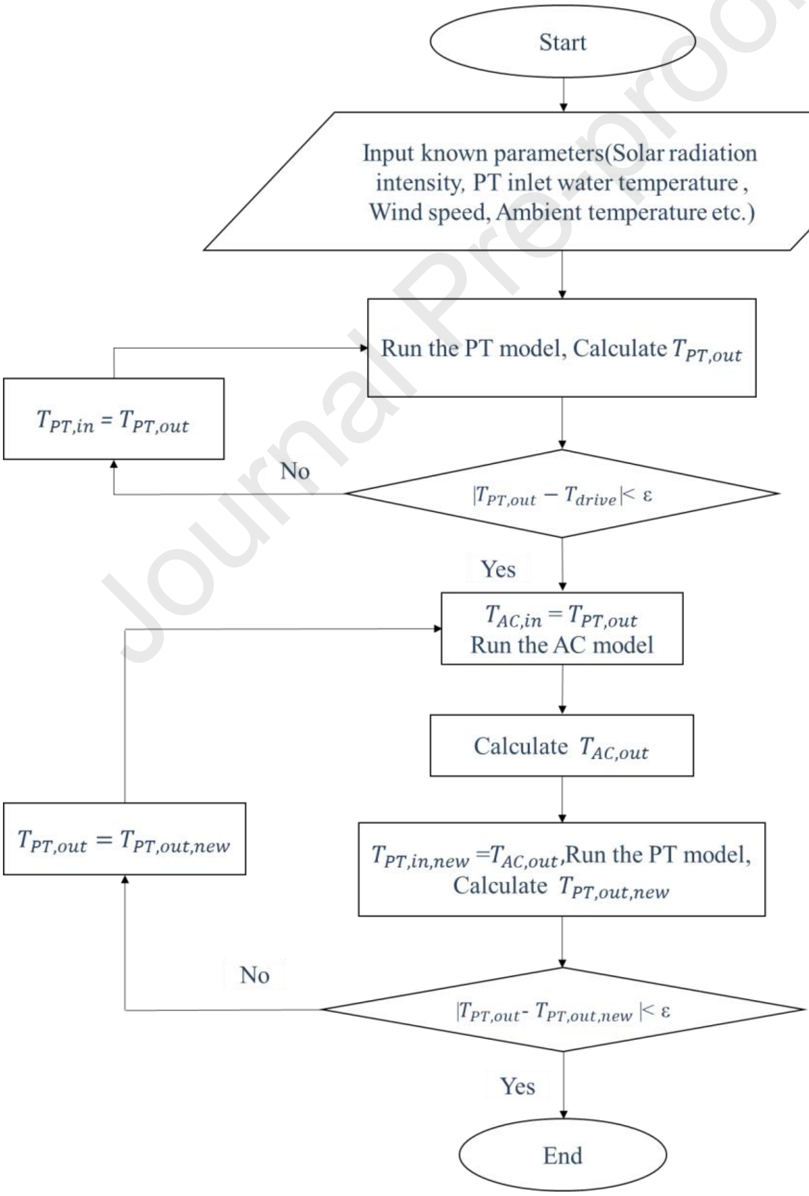

Figure 6: Flow chart of the calculation process for the PT-AC system.

2.4 Thermal load model

To evaluate the performance of the system, a simplified building model is designed to calculate its thermal load, which is later used as the basis for designing the proposed cooling system. The relevant parameters are shown in Table 3.

Table 3: Parameters of the building space

Parameters	Value
Room dimensions	3.5 m (height) x 10 m (length) x 7 m (width)
Corresponding wall area (A_{wall}), floor area (A_{floor}) and volume of the room (V_{room})	119 m^2, 70 m^2 ， and 245 m^3, respectively
Area of window (A_{win}) that faces south	1.5 m (length)×2 m (width)×3 m^2
The heat transfer coefficient of floor ($\boldsymbol{U_f}$)	1.5$\boldsymbol{W/(m^2 \cdot K)}$

Based on the thermal load model by Khammayom et al. [34], the thermal load Q_L of the room without radiation can be calculated as:

$$Q_L = U_f A_{floor}(-0.3099T_{room} + 0.3867T_{amb}) \qquad (28.)$$

whereas in the daytime, the heat load will be affected by solar radiation through the window. Therefore, we can express Q_L approximately as:

$$Q_L = U_f A_{floor}(-0.3099T_{room} + 0.3867T_{amb}) + \tau_{win}A_{win}I_{v,dir} \qquad (29.)$$

where τ_{win} is the transmittance of the window and is set as 0.95, $I_{v,dir}$ is the incident direct solar irradiation that is perpendicular to the vertical surface. Taken from [35], $I_{v,dir}$ can be expressed as follows:

$$I_{v,dir} = \frac{I_{m,dir} * \cos(\theta)}{\cos(\theta_z)} \qquad (30.)$$

where $I_{m,dir}$ means measured direct solar irradiation (perpendicular to the ground), θ_z and θ represent the angle between the sun's rays and the normal of the ground and vertical surfaces, respectively. These angles can be calculated from the local latitude and longitude, solar time, etc.

3. Model Validation

3.1 Absorption chiller model validation

The AC model is executed to yield COP results which will be verified in terms of accuracy. Here, the evaporation temperature is 5°C, cooling water temperature of 35°C, and condensation temperature of 40°C. The results are shown in Figure 7, which shows that the COP increases from 0.6 to 0.8 as the generation temperature varied from 80□ to 110°C. Figure 7 shows the temperature and COP of the single effect absorption chiller.

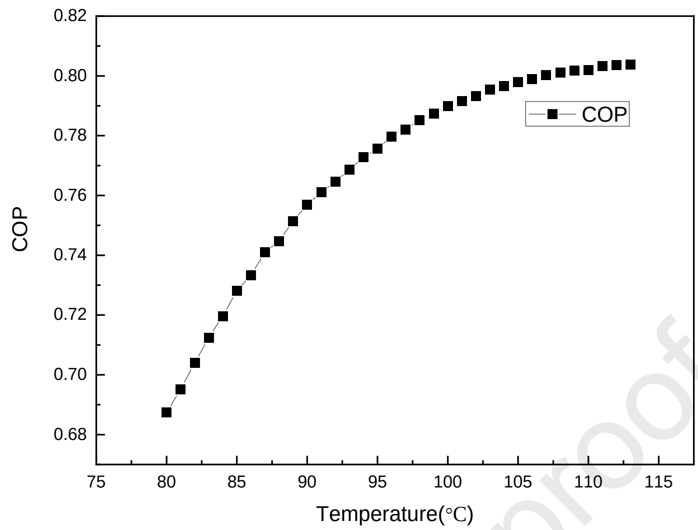

Figure 7: Daily performance of the absorption chiller.

The validation of the AC model is performed with Miao et al. [36], and the comparative results are shown in Table 4. From the chosen five different hot water temperatures, we can see that a good agreement proves that the present model is valid and accepted. Since the model's designed generator temperature is 100°C, which is larger than in the reference, the error gradually increases as the temperature increases.

Table 4: Validation result of AC model

Hot water temperature	COP from Ref.[36]	COP from the present model	Error (%)
85	0.7156	0.7281	1.72
87	0.72772	0.74103	1.80
90	0.73827	0.7569	2.46
92	0.74388	0.76865	2.90
95	0.74568	0.7757	3.87

3.2 Radiative sky cooling model validation

Zhao et al.[10] calculated and tested the net radiation heat flux of selective surface for various surface temperatures. In their study, all tests were under the condition that the surface temperature is close to the ambient temperature to eliminate the convective and conductive heat transfer between the radiative cooling surface and the ambient. These same conditions have been applied to our model from Section 2.1, and the comparison of the results with Zhao et al. is shown in Figure 8 (a). The error between the two may be due to differences in atmospheric transmittance. But overall, the comparison shows that the model in this paper is in good agreement with the references. The average relative error is about 5.36%, therefore, we believe that the RSC model in this study is reliable and accurate.

3.3 Photothermal model validation

Gao et al.[37] has carried out an experimental study on the related properties of the evacuated flat plate collector. In their study, a medium-scale thermal system was used to obtain the output water temperature at different input water temperatures and solar irradiation with the ambient temperature of 35.7℃. Under the same working conditions, and assuming that there is no air gap, we simulated the PT model mentioned in section 2.1. The simulation results and the experimental results of Ref.[37] are all shown in Figure 8 (b). The results show that the PT model is reliable.

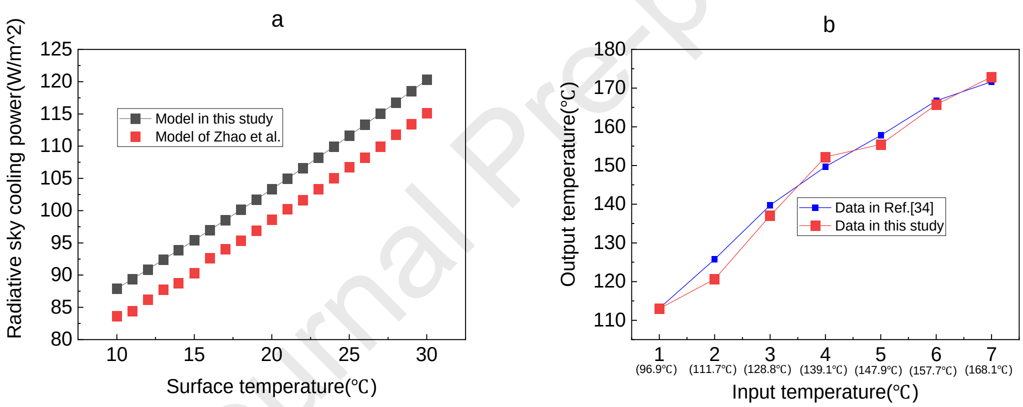

Figure 8: The validation of RSC model (a) and the validation of PT model (b)

4. RESULT AND DISCUSSION

The PT-AC-RSC system has been simulated under varying ambient conditions of the day, and the produced cooling energy is compared with the cooling demand of the building room to evaluate their temporal matching characteristics. First, an analysis using a typical scenario is conducted, which will reveal that the daytime cooling demand is more than that available if the PT-RSC device is sized to exactly meet the nighttime cooling demands. Hence, the performance of the system with a thermal storage tank is evaluated and compared with the traditional PT-AC system. By recognizing the PT-AC-RSC system performs unusually poorly at the sunrise and sunset periods, methods to mitigate the poor performance at these times are proposed and analyzed. Finally, the stability of the PT-AC-RSC system under multiple days with different weather conditions is conducted.

4.1 Preliminary analysis

Base case results are reported below, where the cooling space temperature (T_{room}) is first fixed at the target of 27□, and the ambient temperature, ambient RH, and magnitude of solar irradiance are all varied according to Hefei's weather data on August 1. The area of the PT panel is assumed to be $A_s = 30\ m^2$. It is assumed that the surface temperature of the PT plate is almost equal to room temperature ($T_s \approx T_{room}$) when the system is operating in RSC mode. The convective heat-transfer coefficient h_{bi} between the absorber and bottom plates is set as 1 $\mathrm{W/(m^2\ K)}$ at daytime, that is, the air gap is set as 3 cm.

The all-day cooling energy is shown in Figure 9, including the radiation sky cooling energy at night and the absorption chiller cooling energy at daytime. Clearly, the cooling energy of RSC is about 50~100W/m^2 and depends on the ambient temperature. In the daytime, the cooling capacity of the AC varies with a similar trend to that of the solar radiation intensity, which first increases and then decreases. There are periods in the sunrise and sunset in which the cooling capacity of the system is low. These periods shall be named the "Alternating period of refrigeration (APR)". During these times, T_{amb} is too high and there's too much convective heat loss. Meanwhile, the PT panel will inevitably absorb some solar radiation. However, at the same time, the solar radiation is also too weak to heat the water to the required driving temperature by the AC. Therefore, we can find that the cooling capacity of the RSC at sunset is lower than that at sunrise because of higher solar irradiation and ambient temperature.

By the heat load model mentioned in section 2.4, we also simulated the heat load on August 1 based on Hefei's weather data. I is the solar radiation density. The calculation results of all-day thermal load are also shown in Figure 9. These results indicate that the cooling energy generated by the new system is roughly equal to an entire day's heat load. Among them, the AC model performs very well, showing sufficient cooling capacity. However, during the sunset, the cooling capacity of daytime RSC is somewhat inadequate because the ambient temperature is still very high to cause a high thermal load and low cooling capacity of RSC. Hence, the APR is a very significant problem and a more detailed analysis shall be conducted in Section 4.2 to find solutions to reduce its impact on the time of insufficient cooling capacity.

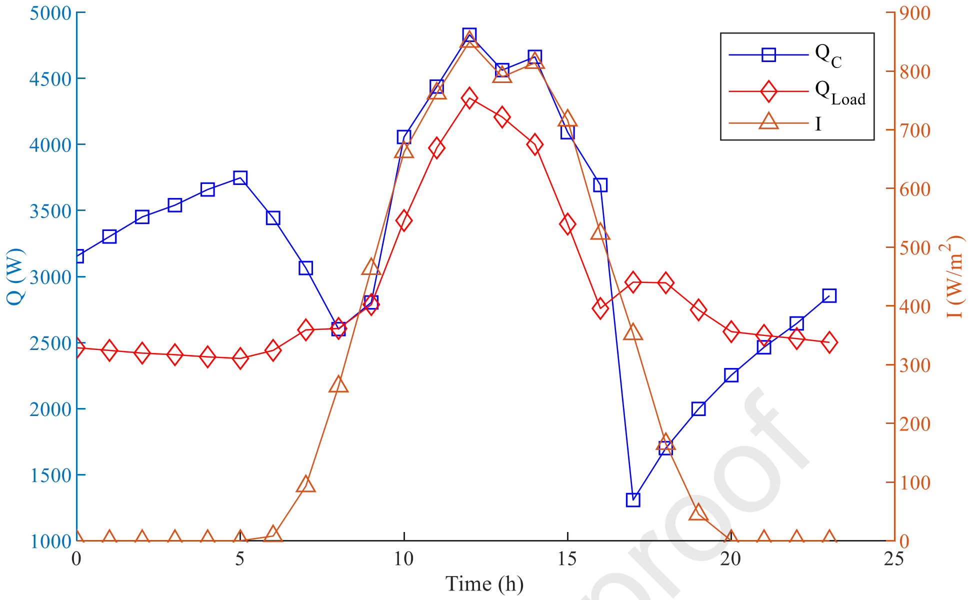

Figure 9: Cooling energy of PT-AC-RSC system and heat load with the time on August 1

4.2 Solutions to reduce the alternating period of refrigeration

As shown by the analysis in Section 4.1, the presence of the APR problem is bound to affect human comfort. This problem can be solved by considering two aspects. The first is to increase the output water temperature $T_{f,o}$ by improving the thermal efficiency η_{PT} of the PT device. Due to the heat transfer coefficient h_{bi} is a very important influential factor on the PT panel's thermal efficiency, so methods to minimize it will be determined.

4.2.1 Influence of heat transfer coefficient h_{bi}

The solar radiation intensity is first simulated based on the summer solstice in Hefei. Under this condition, the effect of h_{bi} is analyzed, which is equivalent to adjusting the air gaps between the components. As shown in Figure 10, the PT-RSC devices with different heat-transfer coefficient h_{bi} have different cooling capacities. Specifically, at the same irradiation intensity I, the PT-RC device with low heat transfer coefficient h_{bi} can get more cooling energy. On one hand, the PT device has higher thermal efficiency due to the reduction of convective heat loss. On the other hand, because of that, the PT device can attain a higher output temperature $T_{f,o}$, which can also improve the COP of the AC device. This conclusion is consistent with the trends expected from Eq. (26). Similarly, due to the improvement of the system's thermal efficiency, the outlet water temperature of the PT device also reached the driving temperature of AC earlier, thereby reducing the ARP.

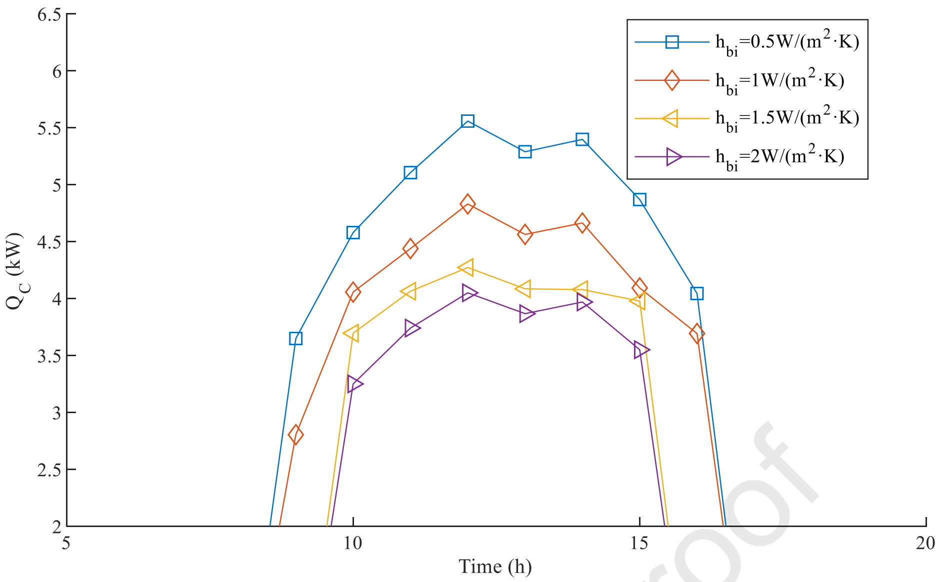

Figure 10: Cooling energy of PT-AC system with different h_{bi}

More specific details are shown in Figure 11, where Figure 11 (a) shows the thermal efficiency of the PT device (PT inlet water temperature equals the ambient temperature) and the driving solar radiation intensity (I_d) of AC (b) under different h_{bi}. From Figure 11 (a), the PT device with lower h_{bi} has a higher η_{PT} under the same solar radiation intensity, especially when the solar radiation intensity is relatively low. From Figure 11 (b), when h_{bi} reaches $2W/(m^2 \cdot K)$, the PT device requires a solar radiation of 584 W/m^2 to heat water to driving temperature. The higher h_{bi} is, the higher solar radiation intensity is needed to drive the AC device. The cutoff solar radiation intensity shows a linear relationship with h_{bi}. The driving solar radiation is $356W/m^2$ when h_{bi} is equal to $0.5W/(m^2 \cdot K)$. This means that at sunrise and sunset, when h_{bi} is 0.5 $W/(m^2 \cdot K)$ compared with 2 $W/(m^2 \cdot K)$, the working time of the PT-AC device can be increased by about 60 minutes. Considering that the data here is discontinuous, the value will be larger.

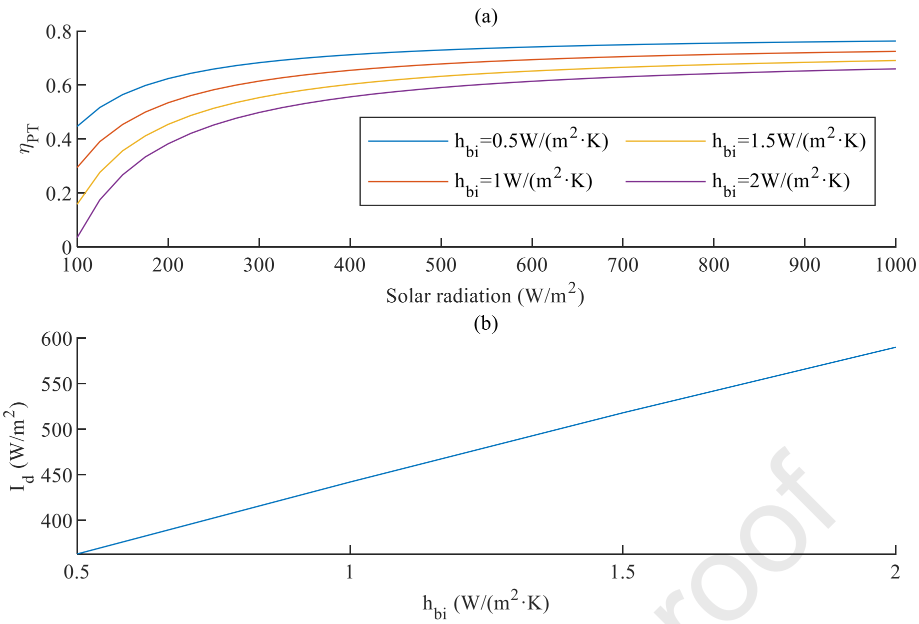

Figure 11: Thermal efficiency η_{PT} of PT-AC system (a) and the cut-off solar radiation intensity of AC (b) with different h_{bi}

Although the above results indicate that a smaller h_{bi} allows a higher PT performance, but a smaller h_{bi} also means the air gap size would need to be larger, which subsequently increases the PT-RSC panel volume and increases its economic cost. Hence, a value of $h_{bi} = 0.5\ W/(m^2 \cdot K)$ is treated as the most reasonable choice and will be used in the next analyzes. Notably, the effect of a low h_{bi} value on the RSC performance is an irrelevant study because, during the nighttime, a blower will be used to enable continuous high airflow rate through the PT-RSC panel, which means the practical h_{bi} value would become significantly high.

4.2.2 Effect of convective heat transfer coefficient on radiative sky cooling

Except decrease the h_{bi} to increase the working time of the PT-AC device, the influence of APR can also be reduced by increasing the cooling energy of the RSC device at night time. Here, the convection heat transfer coefficient between the bottom and the environment is known to be the most influential factor.

As Figure 12 shows, the cooling energy produced by four cases were analyzed: shielded and windless (case 1), shielded and the velocity of wind is $1m/s$ (case 2), without shield and windless (case 3), without shield and $V_{wind} = 1m/s$ (case 4). The results shows that the convection heat transfer coefficient has a major impact on the RSC cooling capacity especially when the ambient temperature is very high. Equation 15 also proves this. In addition, when it is windless and the shield is taken, the APR is reduced by nearly two hours over case 3. Therefore, in the actual situation, measures are needed (such as covering the PE membrane) to reduce the convective heat transfer coefficient as much as possible and ultimately reduce the impact on the RSC.

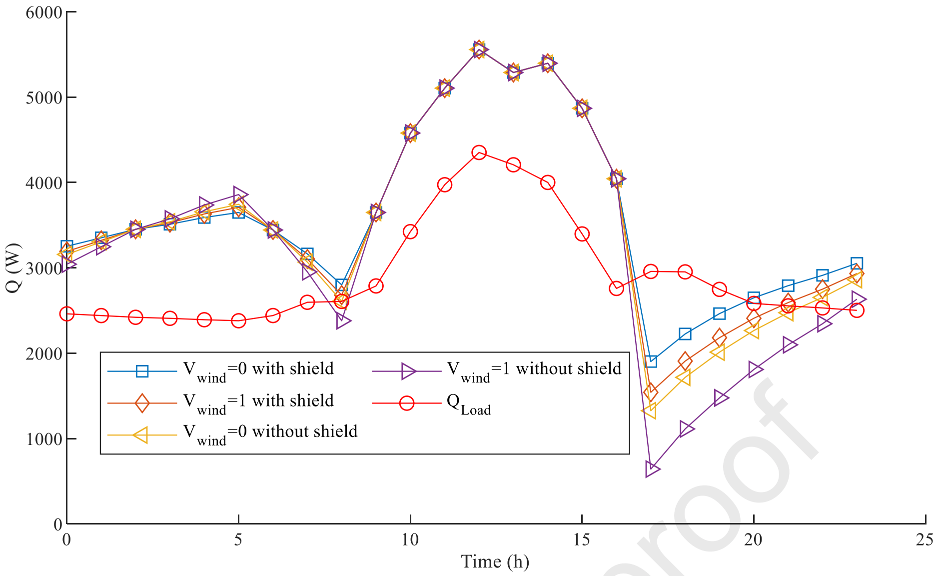

Figure 12: Effects of the different velocity of wind and occlusion measures on system performance

4.3 The system with storage tank

4.3.1 The energy budget of the system

As analyzed above, it is very difficult to completely eliminate the issue under the given cooling area and heat load, which is related to the principle of the RSC itself: The cooling capacity is negatively correlated with the ambient temperature. Similarly, the cooling capacity from dawn to sunrise exceeds the thermal load because of the lower ambient temperature. Therefore, in this section, we analyzed the system with a thermal storage tank and compared it with a separately PT-AC system. The result shows that the new system requires smaller tanks and has greater stability.

Figure 13 shows the solar radiation intensity, the ambient temperature, and cooling capacity of the system for each day of the first week of August, Hefei. Here, h_{bi} is set to 0.5 $W/(m^2 \cdot K)$, assumed that the RSC device was covered with shield and V_{wind} equals to $1m/s$. The trend of system cooling capacity is consistent as mentioned above. Notably, at 5 pm on Day 2, there was an unusually high temperature, which directly caused the RSC to fail to cool.

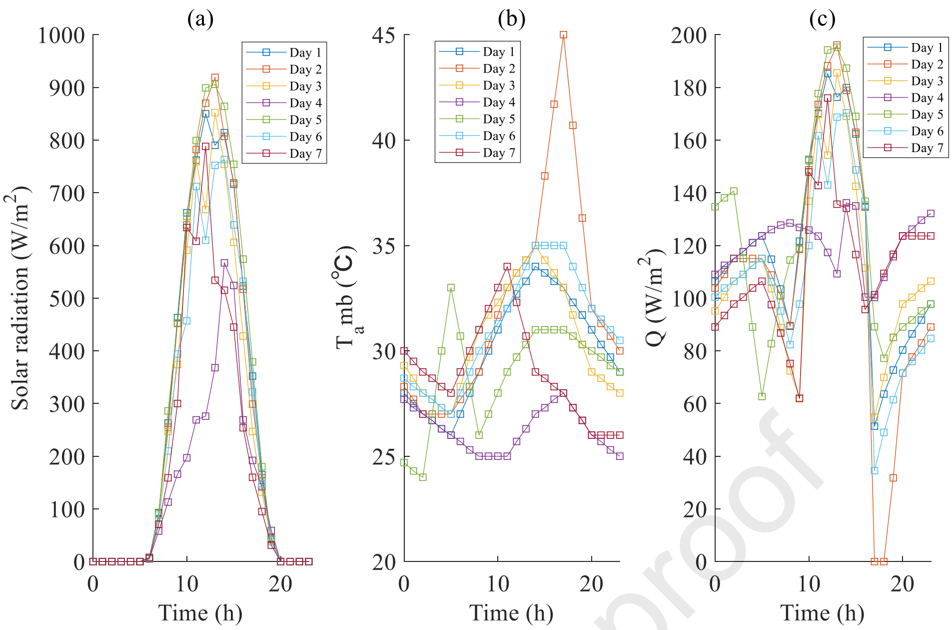

Figure 13: Weather parameters and cooling capacity for one week: solar radiation (a), ambient temperature (b), cooling energy of the system (c)

Consider that the cooling energy produced by AC can be stored as chilling water, it is more convenient and efficient to use than the cooling air produced by RSC. Therefore, it is assumed that only the excess cold energy of AC is stored for use when the cold energy is insufficient. From Figure 14, the amount of stored energy is shown to increase under the original heat load. There is a significant decrease only in about the 40th hour, which is consistent with previous studies. Under the 1.05 times heat load (Case1 E_{Load}), the system can still ensure that the stored energy is always in surplus. At 1.1 times of heat load (Case2 E_{Load}), the energy storage of the system for one week is balanced. Hence, for the original heat load, we consider that the scale of refrigeration is appropriate.

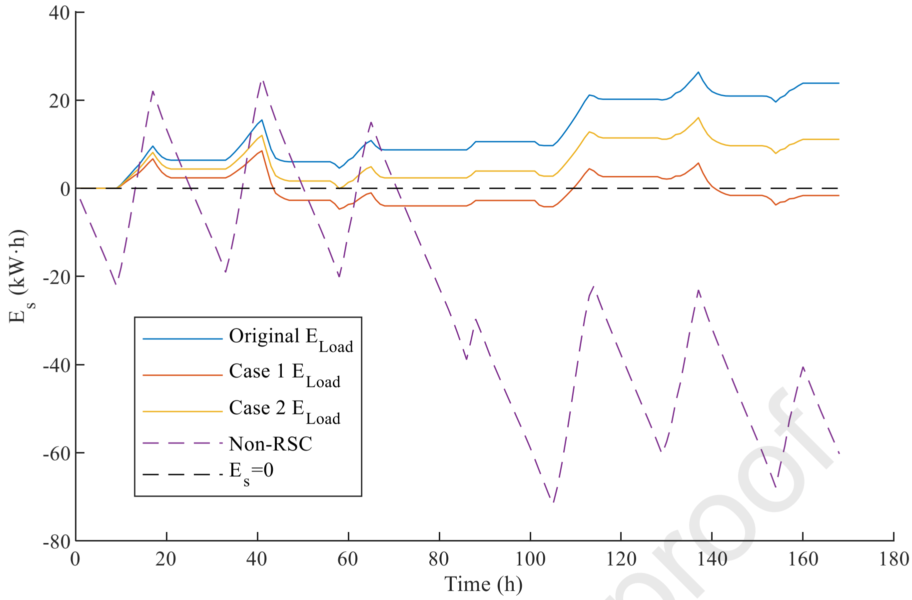

Figure 14: Energy budget of the system in one week.

4.3.2 System performance stability analysis

According to the analysis in section 4.3.1, the new system with a thermal storage capacity of 11.5Kw·h of cooling energy is designed. When the radiation cooling energy can meet the heat load, only the RSC device works. Otherwise, the system will apply the stored cooling energy to satisfy the remaining cooling demands.

Figure 15 (a) shows the cold energy demand of the building and the cooling capacity of the system over the seven days. Here, a surplus of 5% of the cooling abundance for each moment is reserved. The result shows that cooling energy can fit the heat load well. The energy change process of the storage has also been shown in Figure 15 (b). It showed that the stored cooling energy is abundant except on day 2 because the high temperatures that afternoon caused a large heat load.

We also compared the performance of the new system with a separate PT-AC system. The scale of the PT device is redesigned to make sure that the AC cooling energy can satisfy the all-day cooling demand on a sunny day. The energy budget of PT-AC system was also shown in Figure 14 (Non-RSC). It showed that the PT-AC system has much larger energy fluctuations. Besides that, cloudy weather can cause a huge drain on the energy in the tank without replenishment. The PT area and the scale of the storage tank of the two systems are shown in Figure 16. One thing to note is that the PT-AC system does not consider cloudy weather. In fact, the storage tank size is required to meet the maximum energy consumption process of the system. Hence, we can say that the new system can use a smaller storage tank and less floor space to get a more stable refrigeration performance according to the above analysis.

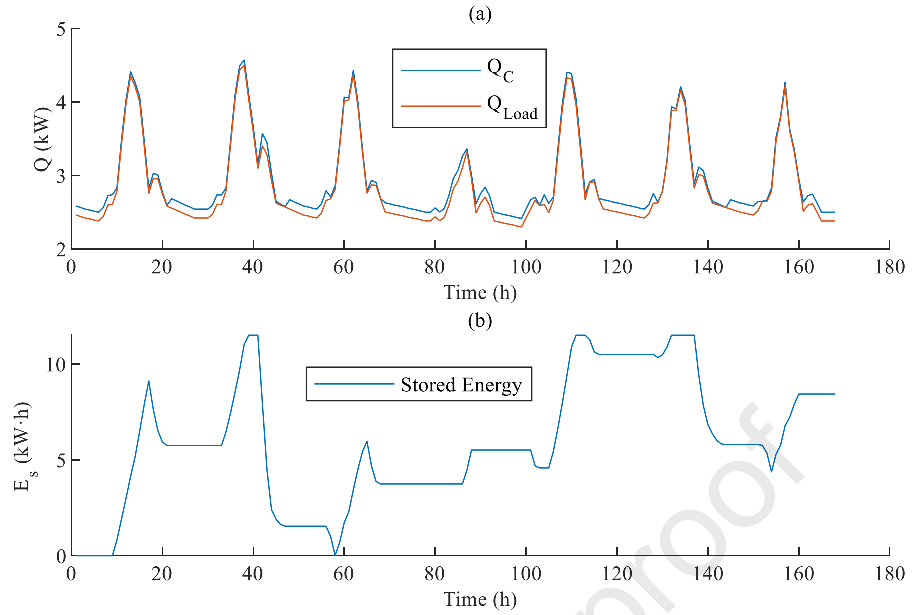

Figure 15: System cooling capacity and building cooling demand for one week

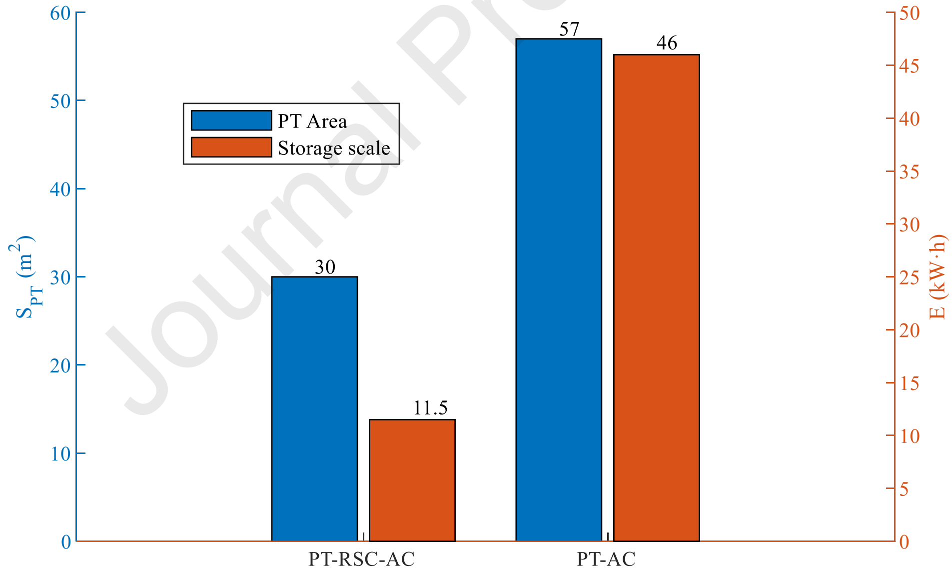

Figure 16: PT area and storage tank scale of PT-AC-RSC system and PT-AC system

4.3.3 Energy analysis

For a more comprehensive evaluation of system performance, the energy output is analyzed for seven days. As shown in Figure 17 the cooling capacity of RSC and AC are similar in quantity. This occurred because the RSC has a much longer working time compared with the AC device. However, there is a huge decrease in AC cooling capacity on day 4. As Figure 13 (a) shows, the solar irradiation on day 4 is lowest this week, so it was estimated that the day might be overcast or cloudy. In contrast, the E_{rsc} is extremely high because of the cooler temperatures of day 4. Therefore, the total cooling energy is relatively adequate compared with heat load on day 4 from Figure 17. It also proved the advantage of the new system: it is more stable to avoid the problems caused by the scarcity of AC cooling capacity. Except for this, the all-day cooling energy matched well with the heat load.

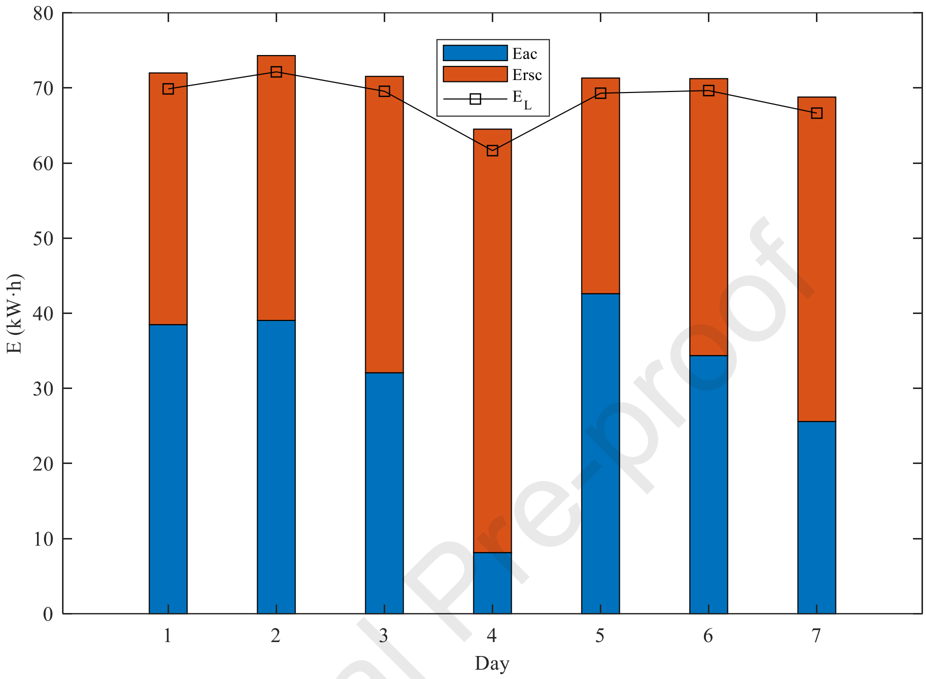

Figure 17: Energy output for one week

5. CONCLUSION

This paper proposed a new all-day cooling system that combined PT-AC with RSC. Based on the vacuum flat plate solar collector, a reversible PT plate with selective absorption coating on the bottom was proposed. This method can significantly reduce the space demand and tank size of the PT-AC system, and improve the economic benefit. In addition, we also find that the new system is more stable and less affected by solar energy fluctuations. More specifically, during the daytime, this new system works like a traditional solar absorption chiller. But at nighttime or when solar radiation is low, such as sunrise and sunset, the PT panels are rotated around to radiate infrared energy for cooling. After simulating this new system via a time-dependent simulation that assumes steady-state characteristics during each hour of the day, it is revealed that:

1. The new system can meet the cooling needs of Hefei during the hottest period. However, weak spots are noticed at the sunrise and sunset periods, a phenomenon which has been named the alternating period of refrigeration (APR).
2. The APR issue can be alleviated by decreasing the heat transfer coefficient h_{bi} via increasing the thickness of the air gap. When h_{bi} is 0.5 $W/(m^2 \cdot K)$, the PT-AC device's working time increases by about 60 minutes at sunrise and sunset

respectively compared with h_{bi} equals to 2 $W/(m^2 \cdot K)$.

3. Also, APR can be further reduced by 2 hours by minimizing the heat transfer coefficient between the bottom and the environment.
4. The new system has a more stable performance than the traditional PT-AC system. The new system only needed an 11.5 kW·h sized thermal storage tank, which is 4 times smaller than the traditional PT-AC system. Moreover, it also correspondingly occupied only half the required floor space.

ACKNOWLEDGMENTS

This research was sponsored by the Fundamental Research Funds for the Central Universities (No. WK2090000021) and the Natural Science Foundation of Hefei, China (Grant No. 2021048).

REFERENCES

1. Heier, J., C. Bales, and V. Martin, *Combining thermal energy storage with buildings – a review.* Renewable and Sustainable Energy Reviews, 2015. **42**: p. 1305-1325.
2. Delzendeh, E., et al., *The impact of occupants' behaviours on building energy analysis: A research review.* Renewable and Sustainable Energy Reviews, 2017. **80**: p. 1061-1071.
3. Olabi, A.G., *Developments in sustainable energy and environmental protection.* Energy, 2012. **39**(1): p. 2-5.
4. Chow, T.T., *A review on photovoltaic/thermal hybrid solar technology.* Applied Energy, 2010. **87**(2): p. 365-379.
5. Wang, R.Z. and X.Q. Zhai, *Development of solar thermal technologies in China.* Energy, 2010. **35**(11): p. 4407-4416.
6. Li, Z., F. Boyle, and A. Reynolds, *Domestic application of solar PV systems in Ireland: The reality of their economic viability.* Energy, 2011. **36**(10): p. 5865-5876.
7. Zhao, D., et al., *Radiative sky cooling-assisted thermoelectric cooling system for building applications.* Energy, 2020. **190**.
8. Ayou, D.S. and A. Coronas, *New Developments and Progress in Absorption Chillers for Solar Cooling Applications.* Applied Sciences, 2020. **10**(12).
9. Vall, S., et al., *A new flat-plate radiative cooling and solar collector numerical model: Evaluation and metamodeling.* Energy, 2020. **202**.
10. Zhao, D., et al., *Radiative sky cooling: Fundamental principles, materials, and applications.* Applied Physics Reviews, 2019. **6**(2).
11. Zeyghami, M., D.Y. Goswami, and E. Stefanakos, *A review of clear sky radiative cooling developments and applications in renewable power systems and passive building cooling.* Solar Energy Materials and Solar Cells, 2018. **178**: p. 115-128.

12. Kim, D.S. and C.A. Infante Ferreira, *Solar refrigeration options – a state-of-the-art review.* International Journal of Refrigeration, 2008. **31**(1): p. 3-15.
13. Ali, A.H.H., P. Noeres, and C. Pollerberg, *Performance assessment of an integrated free cooling and solar powered single-effect lithium bromide-water absorption chiller.* Solar Energy, 2008. **82**(11): p. 1021-1030.
14. Xu, Z.Y. and R.Z. Wang, *Comparison of CPC driven solar absorption cooling systems with single, double and variable effect absorption chillers.* Solar Energy, 2017. **158**: p. 511-519.
15. Azhar, M., M.E. Khan, and M. Meraj, *Performance Analyses of Photovoltaic Thermal Integrated Concentrator Collector Combined With Single Effect Absorption Cooling Cycle: Constant Flow Rate Mode.* Journal of Energy Resources Technology, 2020. **142**(12).
16. Lu, X., et al., *Cooling potential and applications prospects of passive radiative cooling in buildings: The current state-of-the-art.* Renewable and Sustainable Energy Reviews, 2016. **65**: p. 1079-1097.
17. Raman, A.P., et al., *Passive radiative cooling below ambient air temperature under direct sunlight.* Nature, 2014. **515**(7528): p. 540-4.
18. Zhao, D., et al., *Subambient Cooling of Water: Toward Real-World Applications of Daytime Radiative Cooling.* Joule, 2019. **3**(1): p. 111-123.
19. Hu, M., et al., *Comparative analysis of different surfaces for integrated solar heating and radiative cooling: A numerical study.* Energy, 2018. **155**: p. 360-369.
20. Hu, M., et al., *Experimental study on a hybrid photo-thermal and radiative cooling collector using black acrylic paint as the panel coating.* Renewable Energy, 2019. **139**: p. 1217-1226.
21. Mateus, T. and A.C. Oliveira, *Energy and economic analysis of an integrated solar absorption cooling and heating system in different building types and climates.* Applied Energy, 2009. **86**(6): p. 949-957.
22. Eicker, U. and D. Pietruschka, *Design and performance of solar powered absorption cooling systems in office buildings.* Energy and Buildings, 2009. **41**(1): p. 81-91.
23. Said, S.A.M., M.A.I. El-Shaarawi, and M.U. Siddiqui, *Alternative designs for a 24-h operating solar-powered absorption refrigeration technology.* International Journal of Refrigeration, 2012. **35**(7): p. 1967-1977.
24. Ranilović, B. and M. Grozdek, *Potential for Mitigation of Solar Collector Overheating Through Application of Phase Change Materials – A Review.* Journal of Sustainable Development of Energy, Water and Environment Systems, 2020. **8**(4): p. 622-640.
25. CoolProp. *http://www.coolprop.org/.*
26. Bergman, T.L., *Active daytime radiative cooling using spectrally selective surfaces for air conditioning and refrigeration systems.* Solar Energy, 2018. **174**: p. 16-23.
27. Tang, R.S., Y. Etzion, and I.A. Meir, *Estimates of clear night sky emissivity in the Negev Highlands, Israel.* Energy Conversion and Management, 2004.

45(11-12): p. 1831-1843.

28. Zhai, Y., et al., *Scalable-manufactured randomized glass-polymer hybrid metamaterial for daytime radiative cooling.* Science, 2017. **355**(6329).
29. *https://energyplus.net/weather*.
30. Zhao, D.L., et al., *Subambient Cooling of Water: Toward Real-World Applications of Daytime Radiative Cooling.* Joule, 2019. **3**(1): p. 111-123.
31. Huang, Z. and X. Ruan, *Nanoparticle embedded double-layer coating for daytime radiative cooling.* International Journal of Heat and Mass Transfer, 2017. **104**: p. 890-896.
32. Bergman, T.L., Lavine, A.S., *Fundamentals of Heat and Mass Transfer, eighth ed.* 2017.
33. Handbook, A., *https://www.ashrae.org/.* 2013.
34. Khammayom, N., N. Maruyama, and C. Chaichana, *Simplified model of cooling/heating load prediction for various air-conditioned room types.* Energy Reports, 2020. **6**: p. 344-351.
35. Kim, S., et al., *Design optimization of large-scale attached cultivation of Ettlia sp. to maximize biomass production based on simulation of solar irradiation.* Applied Energy, 2020. **279**.
36. *<Simulation on single-effect lithium bromide absorption refrigerator.pdf>*.
37. Holman, J., *Heat Transfer. 10th.* Boston, MASS. McGraw-Hill. , 2010.

Highlights

- A new system combined AC and RSC is proposed to realize 24-h continuous cooling at smaller space and thermal storage.
- The steady-state model of this system is analyzed and compared with the traditional PT-AC.
- This system can meet the room heat load during most of the day except sunset.
- The performance can be improved significantly by reducing the convection and conduction heat loss.
- This system only needed a 4 times smaller thermal storage tank and half the floor space.

Declaration of interests

☒ The authors declare that they have no known competing financial interests or personal relationships that could have appeared to influence the work reported in this paper.

☐The authors declare the following financial interests/personal relationships which may be considered as potential competing interests: